

Electronic Supplementary Material

Self-powered and Low-temperature Resistant MXene-modified Electronic-skin for Multifunctional Sensing

Minmin Wang^{a,b,†}, Weiqun Liu^{a,†}, Xu Shi^a, Yafei Cong^a, Shuai Lin^a, Tongming Sun^{a, b,*}, Jin Wang^{a, b,*}, and Yanfeng Tang^{a, b,*}

^a School of Chemistry and Chemical Engineering, Nantong University, Nantong 226019, China.

^b Nantong Key Laboratory of Intelligent and New Energy Materials, Nantong University, Nantong 226019, China.

*Corresponding authors' E-mail:

Tongming Sun: stm7314@ntu.edu.cn;

Jin Wang: wangjin110@ntu.edu.cn;

Yanfeng Tang: tangyf@ntu.edu.cn.

† These authors contributed equally to this work.

Experimental Section

Material

Lithium fluoride (LiF) was purchased from Shanghai Yien Chemical Technology Co., Ltd. Titanium aluminum carbide powder (Ti_3AlC_2 , $M_w \sim 195$ Da, 325 mesh) was purchased from Forsman Technology (Beijing) Co., Ltd. Sodium carboxymethylcellulose (CMC, $M_w \sim 90$ kDa) was purchased from Shanghai Jierun Chemical Reagent Co., Ltd. 2, 2'-bis[2-(2-imidazolin-2-yl)propane] dihydrochloride (AIBI, $M_w \sim 323$ Da), Acrylamide (AAM, $M_w \sim 71$ Da), Tannic acid (TA, $M_w \sim 1701$ Da), Tris (hydroxymethyl) methyl aminomethane (THAM, $M_w \sim 121$ Da), and Glycerol were purchased from Aladdin. Disodium tetraborate decahydrate ($M_w \sim 381$ Da) was purchased from Shantou Xilong Chemical Factory Co., Ltd. N, N'-methylene diacrylamide (MBAA) was purchased from Yanfeng Technology (Beijing) Co., Ltd. PDMS prepolymer and curing agent were purchased from Dow Corning. The water used in all experiments was ultrapure (18.20 M Ω .cm). All chemicals were used as received and without any further purification.

Synthesis of $\text{Ti}_3\text{C}_2\text{T}_x$ nanosheets

$\text{Ti}_3\text{C}_2\text{T}_x$ nanosheets were synthesized by selectively etching the Al layer of Ti_3AlC_2 and then peeling off. In detail, 1.5 g LiF was dissolved in 30 mL HCl (9 M). Then, 1.5 g Ti_3AlC_2 was slowly transferred into the above mixed solution in an ice bath, and the etching reaction was continued to stir at 45 °C for 24 h. Subsequently, the obtained product was centrifuged several times and washed with deionized water until the pH of the supernatant was 6 (5000 rpm for 20 min per cycle). Then, the low turbidity liquid was dispersed to deionized water by ultrasound under the protection of N_2 . Finally, the layered dark green supernatant was collected with a pipette, and $\text{Ti}_3\text{C}_2\text{T}_x$ nanosheets were obtained by freeze-drying for 10 h.

Preparation of PDMS based single electrode

The PDMS prepolymer was fully mixed with the curing agent with a mass ratio of 10:1 under stirring. Then, the mixed solution was poured into a mold equipped with metal flakes (2 cm \times 2 cm \times 0.3 mm), and the thickness of the film was controlled by a doctor blade. Then, a PDMS based mold (3 cm \times 3 cm \times 0.5 mm) with a cavity (2 cm \times 2 cm \times 0.3 mm) was obtained by drying at 90 °C for 2 h. In addition, a PDMS film (2 cm \times 2 cm \times 0.2 mm) without cavity was also obtained by the same way without using the metal flakes.

Synthesis of $\text{Ti}_3\text{C}_2\text{T}_x$ nanosheets embedded freeze-resistant hydrogel

Synthesis of hydrogel comes from a modification of reported works.¹⁻³ The freeze-resistant hydrogel initial solution was prepared as follow steps. First, 0.014 g TA was added to 5.0 g CMC dispersion (0.9 wt%) and the pH was adjusted to 8.1 by dropping 1 M Tris-HCl buffer solution. The mixture was stirred at room temperature for 8 hours to obtain TA@CMC suspension. Then, 3.0 g $\text{Ti}_3\text{C}_2\text{T}_x$ nanosheets aqueous solution (1.2 wt%), 6.0 g AAM powder, 400

μL MBAA solution (15 wt%), 90 μL AIBI solution (2 wt%), and 5 g glycerin (GL) were added to the above TA@CMC suspension with stirring. And then, 600 μL of sodium borohydride solution (6 wt%) dropped into the above solutions. Finally, the mixed solution was stirred for 10 minutes to fully dissolve, and deoxygenated under vacuum for 10 min to obtain the $\text{Ti}_3\text{C}_2\text{T}_x$ nanosheets embedded freeze-resistant hydrogel initial solution.

Fabrication of freeze-resistant e-skin

First, the above obtained hydrogel initial solution was transferred to a PDMS mold containing a cavity and then coated with a plastic wrap to prevent water volatilization. Second, ultraviolet radiation (250 W, 365 nm) was used for 10 min to induce copolymerization to form an organic hydrogel in situ. Then, another as-prepared thin PDMS film attached to the mold, and connected to a conductive copper wire, sealed with a PDMS solution, and left at room temperature for seven days to obtain the e-skin.

Characterization

The stress and strain of the hydrogel and e-skin were measured using a computer controlled universal electronic tensile testing machine (CMT7104). The field emission scanning electron microscope (Gemini SEM 300) and transmission electron microscope (JEM-2100) were used to observe the detail morphology of the hydrogel. The physical phase of the as-prepared $\text{Ti}_3\text{C}_2\text{T}_x$ nanosheets was examined by powder X-ray diffraction (AXS D8 Advance).

Electrical Measurement

A vibration exciter (HEAS-20) was used to simulate contact pressure and frequency. The conductivity of hydrogels was measured by the alternating current impedance method at the electrochemical workstation (CHI 660E). The natural environment of the e-skin is simulated through the freezer (BCD-325WDGB), cryopreservation box (DW-45W28), and constant temperature oven (DHG-9076A). During the test, the skin was replaced by an ethylcellulose film for typical electrical measurements. A digital phosphor oscilloscope (Tektronix MDO3014) and a low noise current preamplifier (Stanford SR570) were used to collect the voltage and current signals of the e-skin ($2 \times 2 \text{ cm}^2$).

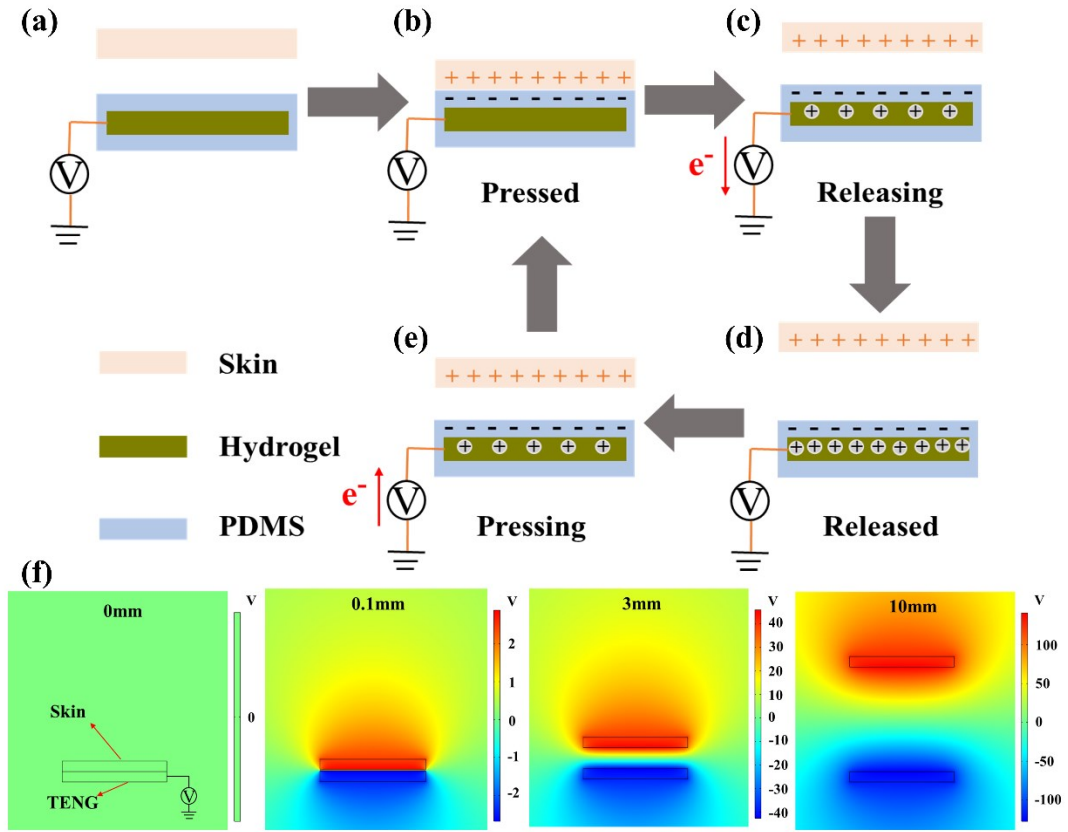


Fig. S1. (a-e) The working principle of self-powered e-skin. (f) The voltage simulation of the e-skin.

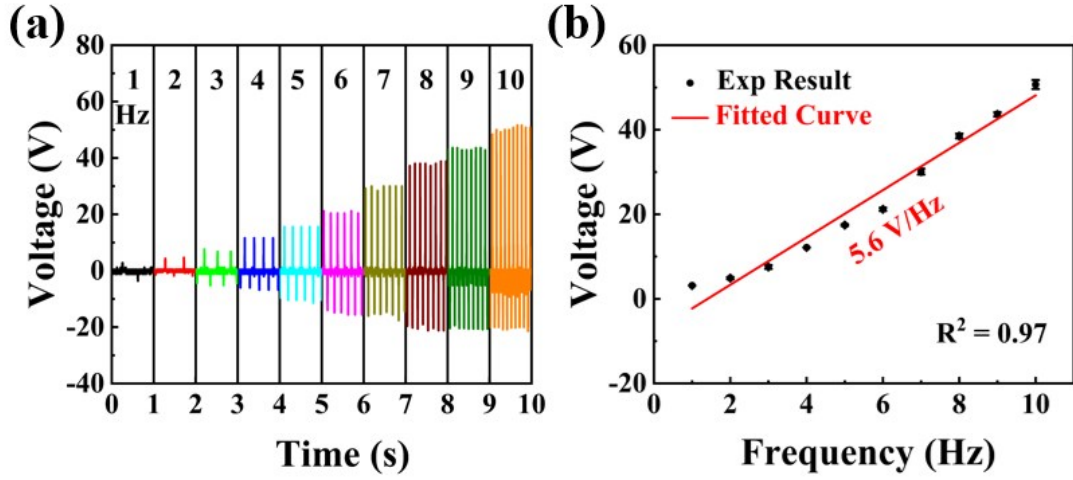


Fig. S2. (a) The V_{oc} of the e-skin at various frequency at a low ambient temperature (-15 °C) and (b) the corresponding limit of detection of the frequency of the developed e-skin.

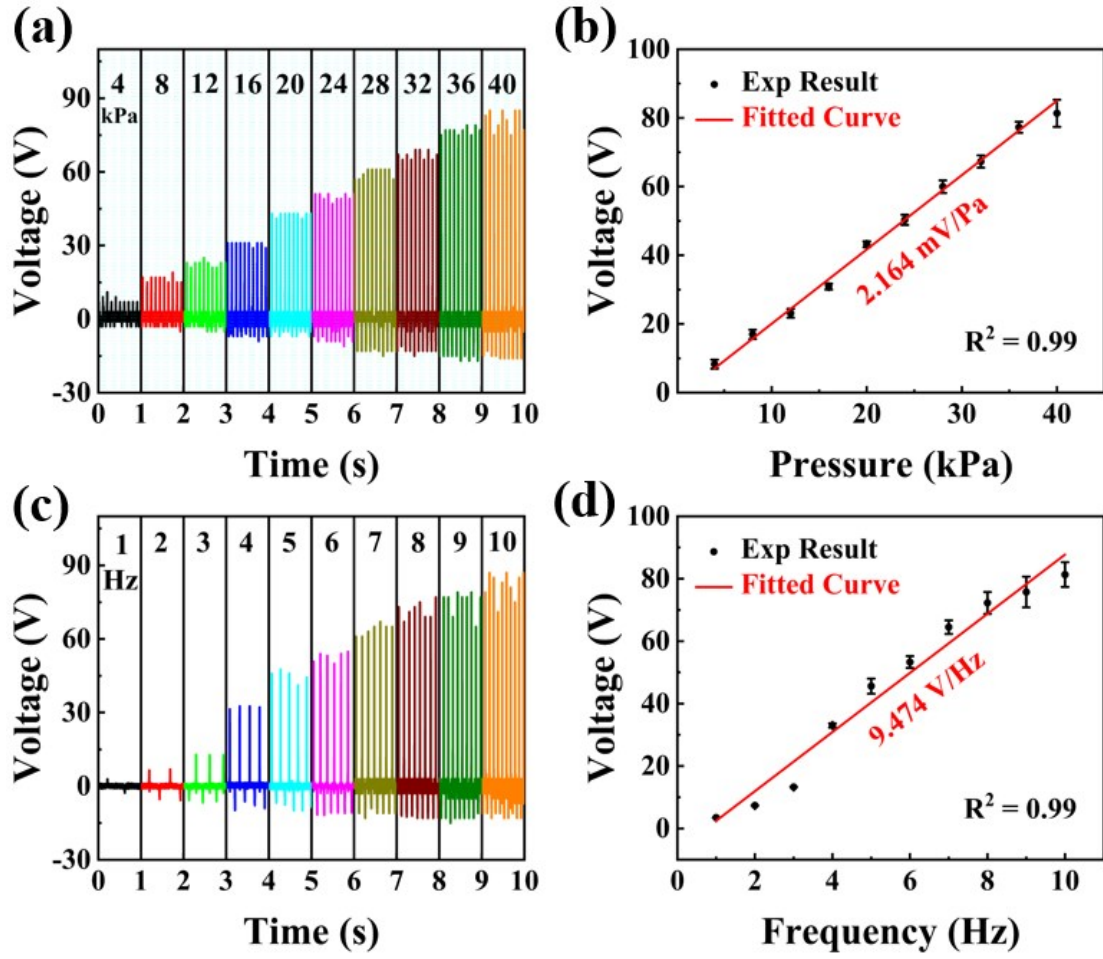


Fig. S3. (a) The V_{oc} of the e-skin at various pressure at a normal ambient temperature (25 °C) and (b) the corresponding limit of detection of the pressure of the developed e-skin (measured at a fixed frequency of 10 Hz) ($L = 41.59 \text{ Pa}$). (c) The V_{oc} of the e-skin at various frequency at a normal ambient temperature (25 °C) and (d) the corresponding limit of detection of the frequency of the developed e-skin (measured at a fixed pressure of 0.040 MPa) ($L = 0.0095 \text{ Hz}$).

Table. S1. Sensitivity summary of e-skin with different structures and electrodes.

Triboelectric layer	Electrode	Working mode	structure	Sensitivity (mV Pa ⁻¹)	Contact area (cm ²)	Ref.
PDMS film	Graphene	single	mesh	0.274	0.2	4
PDMS film	PAAm-LiCl hydrogel	single	sandwich	0.013	12	5
PDMS film	PEDOT:PSS film	single	wrinkled	0.08	18	6
PDMS film	rGO/BiTO/PVDF	single	pyramidal	5.07	1.5	7
PDMS film	Cu	contact-separate	micro-frustum - array	0.0567	3.6	8
PDMS film	Cu	single	sandpaper	0.367	-	9
PDMS film	MXene-GL-hydrogel	single	sandwich	2.164 (25 °C)	4	This work
PDMS film	MXene-GL-hydrogel	single	sandwich	1.29 (-15 °C)	4	This work

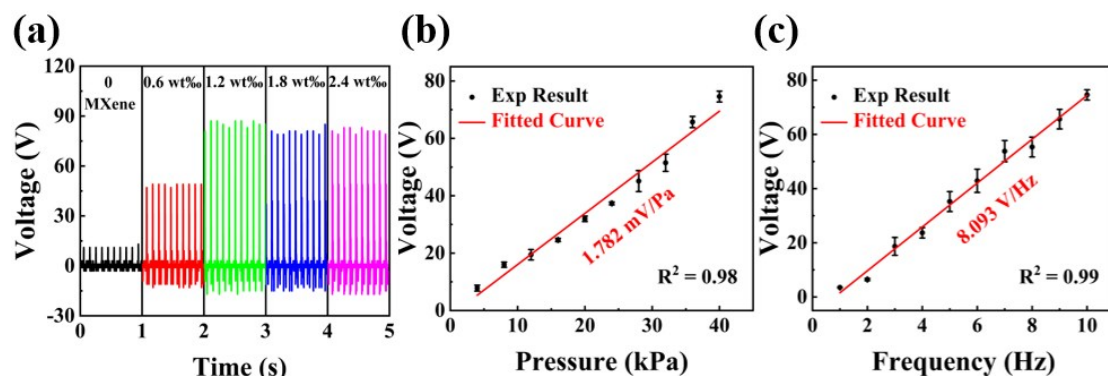


Fig. S4. (a) Output performance of e-skin based on different doping content of MXene (b) The relationship between the open-circuit voltage (V_{oc}) of the e-skin to pressure (2.4 wt%). (c) The relationship between the open-circuit voltage (V_{oc}) of the e-skin to frequency (2.4 wt%).

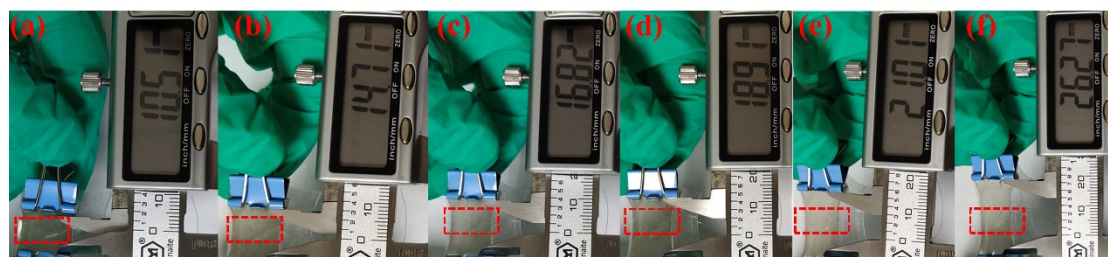


Fig. S5. The photograph of the e-skin stretched to various strains, (a) 0%, (b) 40%, (c) 60%, (d) 80%, (e) 100%, and (f) 150%.

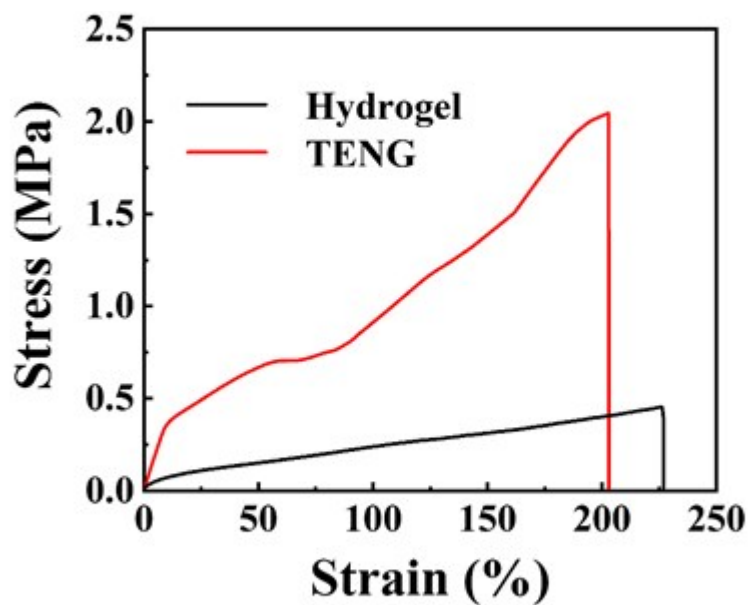


Fig. S6. Uniaxial tensile test of as-prepared hydrogel and developed e-skin.

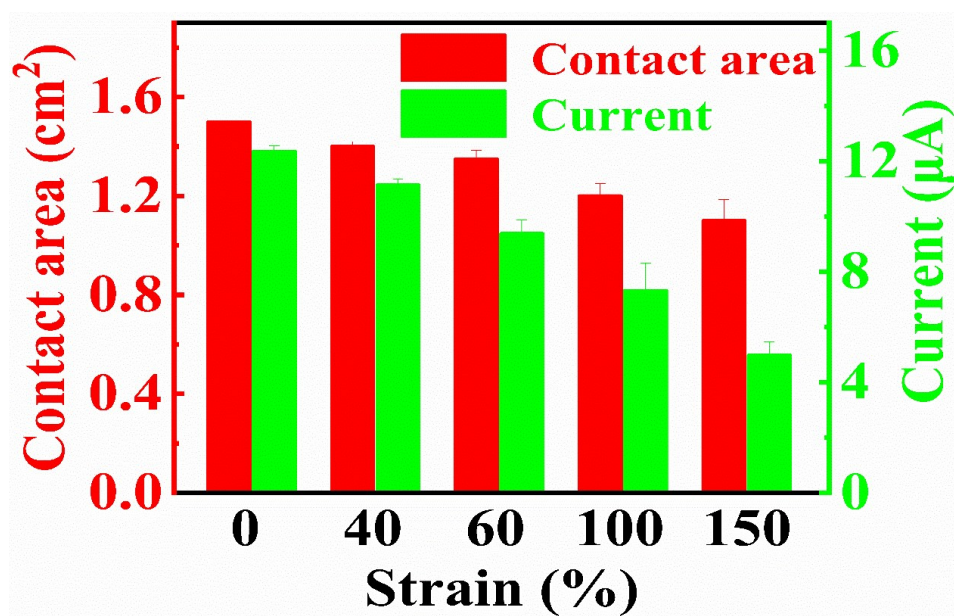


Fig. S7. The contact area and output current for our developed e-skin under various strains.

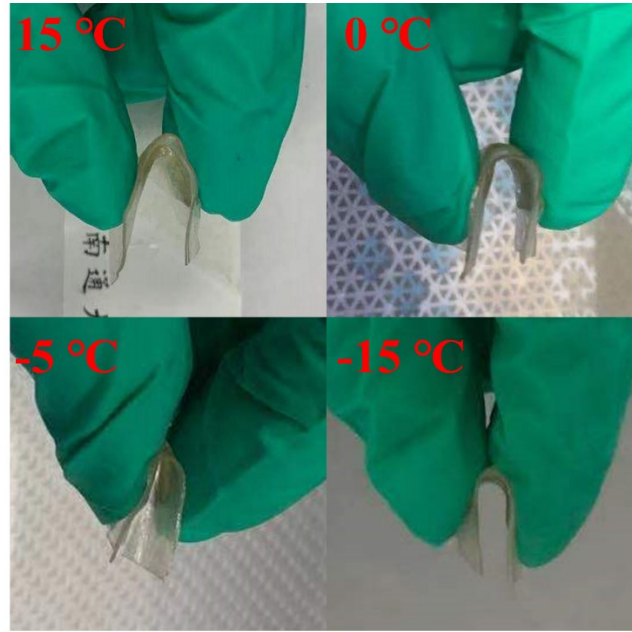


Fig. S8. Photographs of the flexibility of the developed e-skins at different temperature environments.

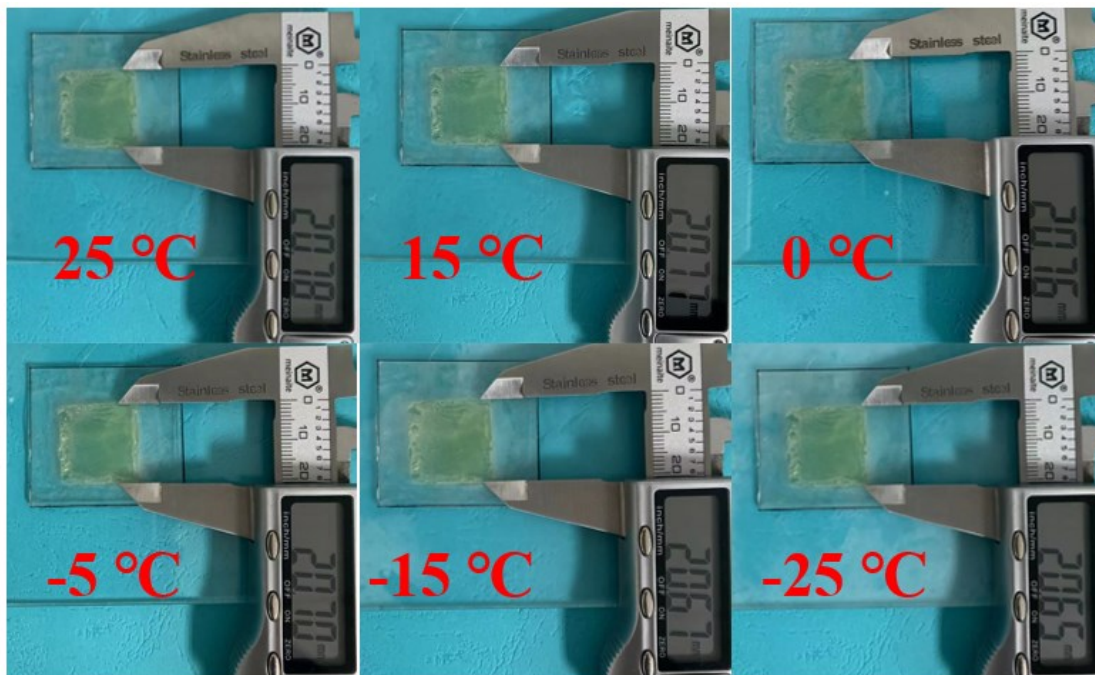


Fig. S9. Photographs of the shrinkage effect of electronic skin affecting the contact area at different temperatures.

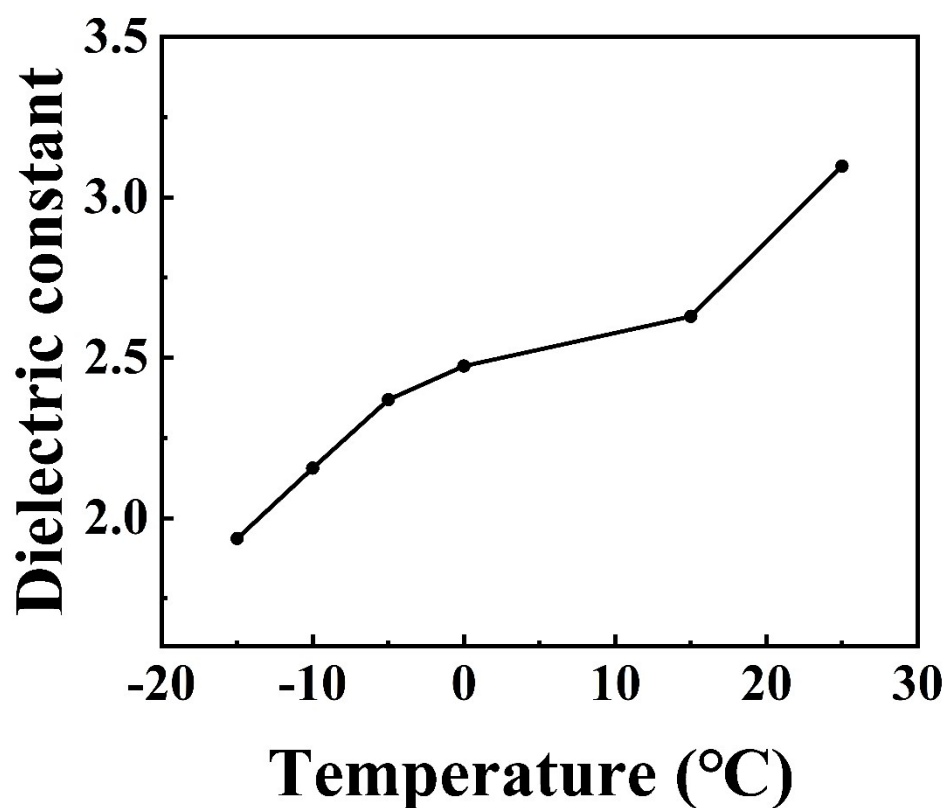


Fig. S10. The relationship between the dielectric constant of the PDMS film and the temperature (1 MHz).

Table. S2. Comparison of the stretchability of the developed e-skin with the most recently reported PDMS based e-skins at a low ambient temperature.

Triboelectric layer	Electrode	Working mode	Application temperature	stretchability	Ref.
PDMS film	PAAm-LiCl hydroge	single	0 °C ~	400%	5
PDMS film	rGO/BiTO /PVDF	single	25 °C ~	-	7
PDMS film	Cu	single	25 °C ~	42%	9
PDMS and PANI film	Cu	contact-separate	36.5 °C ~	-	10
PDMS film	GO dispersion	single	0 °C ~	275%	11
PDMS film	MXene-GL-hydrogel	single	-15 °C ~	200%	This work

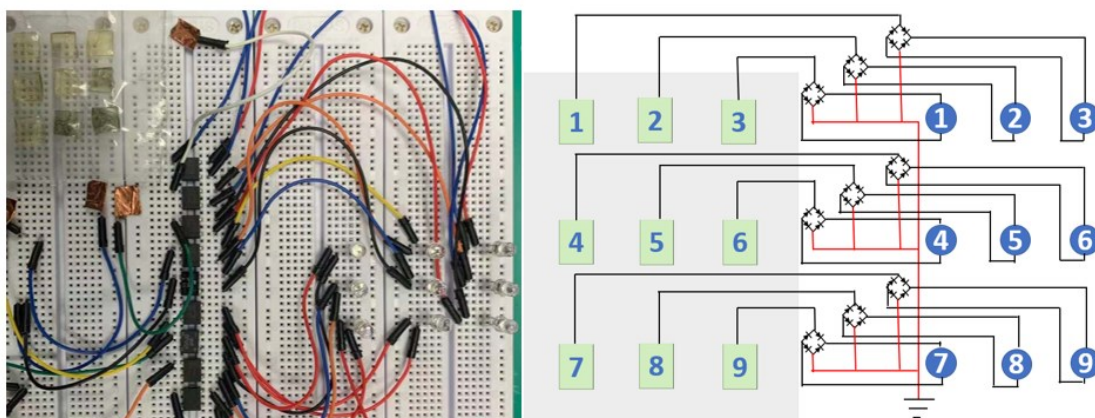


Fig. S11. Circuit diagram of the self-powered e-skin array for lighting up the LEDs.

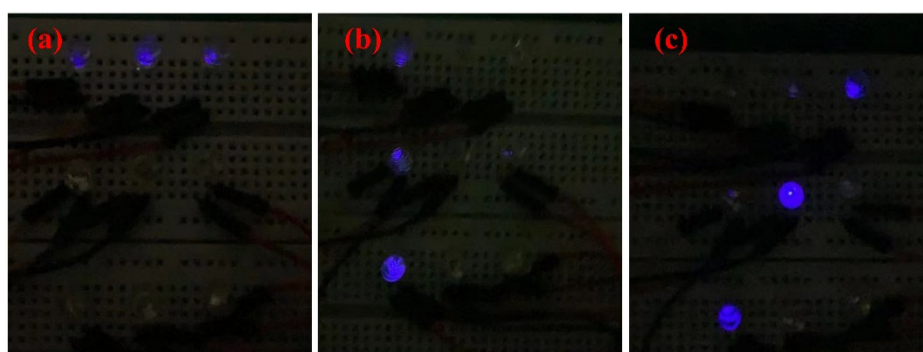


Fig. S12. Photographs of the e-skin array in lighting up the LEDs at various temperatures, (a) 15 °C, (b) 0 °C, (c) -15 °C.

Notes and references

1. Y. Wei, L. Xiang, H. Ou, F. Li, Y. Zhang, Y. Qian, L. Hao, J. Diao, M. Zhang, P. Zhu, Y. Liu, Y. Kuang and G. Chen, *Adv. Funct. Mater.*, 2020, **30**, 2005135.
2. K. H. Lee, Y.-Z. Zhang, Q. Jiang, H. Kim, A. A. Alkenawi and H. N. Alshareef, *ACS Nano*, 2020, **14**, 3199-3207.
3. Y. Cai, J. Shen, C.-W. Yang, Y. Wan, H.-L. Tang, A. A. Aljarb, C. Chen, J.-H. Fu, X. Wei, K.-W. Huang, Y. Han, S. J. Jonas³, X. Dong and V. Tung, *Sci. Adv.*, 2020, **6**, eabb5367.
4. Y. Lee, J. Kim, B. Jang, S. Kim, B. K. Sharma, J.-H. Kim and J.-H. Ahn, *Nano Energy*, 2019, **62**, 259-267.
5. P. Xiong, L. Mengmeng, C. Xiangyu, S. Jiangman, D. Chunhua, Z. Yang, Z. Junyi, H. Weiguo and W. Z. Lin, *Sci. Adv.*, 2017, **3**, e1700015.
6. Y. Yang, N. Sun, G. Li, Y. Liu, C. Chen, J. Shi, L. Xie, H. Jiang, D. Bao, Q. Zhuo and X. Sun, *Adv. Funct. Mater.*, 2018, **28**, 1803684.
7. J. Rao, Z. Chen, D. Zhao, R. Ma, W. Yi, C. Zhang, D. Liu, X. Chen, Y. Yang, X. Wang, J. Wang, Y. Yin, X. Wang, G. Yang and F. Yi, *Nano Energy*, 2020, **75**, 105073.
8. J. Yu, X. Hou, J. He, M. Cui, C. Wang, W. Geng, J. Mu, B. Han and X. Chou, *Nano Energy*, 2020, **69**, 104437.
9. J. He, Z. Xie, K. Yao, D. Li, Y. Liu, Z. Gao, W. Lu, L. Chang and X. Yu, *Nano Energy*, 2021, **81**, 105590.

10. Z. Liu, T. Zhao, H. Guan, T. Zhong, H. He, L. Xing and X. Xue, *J. Mater. Sci. Technol.*, 2019, **35**, 2187-2193.
11. Y. Wu, Y. Luo, J. Qu, W. A. Daoud and T. Qi, *Nano Energy*, 2019, **64**, 103948.